DOI 10.1007/s11041-015-9814-5
Metal Science and Heat Treatment, Vol. 56, Nos. 11 – 12, March, 2015 (Russian Original Nos. 11 – 12, November – December, 2014)

CORROSION-RESISTANT AND SOFT-MAGNETIC ALLOYS

UDC 620.186.1:669.018.8

SPECIAL FEATURES OF FORMATION OF EXCESS PHASES DURING AGING OF CORROSION-RESISTANT HIGH-ALLOY AUSTENITIC ALLOYS BASED ON Fe AND Ni

S. V. Belikov,[1] A. Yu. Zhilyakov,[1] A. A. Popov,[1] M. S. Karabanalov,[1] and I. B. Polovov[1]

Translated from *Metallovedenie i Termicheskaya Obrabotka Metallov*, No. 12, pp. 3 – 11, December, 2014.

The applicability of the active criteria for estimating the metastability of austenite for predicting the operating capacity of high-alloy corrosion-resistant alloys based on iron and nickel in a single-phase preliminarily quenched condition in a temperature range of up to 500 – 650°C is analyzed. The temperature and time ranges of formation of excess phases are determined and fragments of *C*-curves are plotted. The effect of preliminary cold plastic deformation on the kinetics of aging and on the morphology of segregation of particles of second phases is studied.

Key words: high-alloy corrosion-resistant alloys, excess phases, aging.

INTRODUCTION

Successful development of the chemical industry, nonferrous metallurgy and power engineering demands advancement of structural materials, in particular, a satisfactory corrosion-resistance in molten salts at elevated (over 350°C) temperatures.

The most corrosion-resistant austenitic alloys based on iron and nickel with additives of chromium and molybdenum can serve in aggressive environments containing F^-, Cl^-, SO_3^-, and H_2S at up to 120°C. These alloys have been designed for operation in a hardened condition with a structure of supersaturated γ-solid solution and a low content of carbides or carbonitrides of type MeC/Me(C, N). A minimum content of second phases provides enhanced resistance to electrochemical corrosion, and transition of the alloying elements into the austenitic matrix promotes formation of dense protective oxide films in oxidizing corrosive environments and provides solid-solution hardening of the matrix. After quenching, these alloys are not susceptible to natural aging, but elevation of the service temperature causes a diffusion redistribution of atoms, which affects negatively the stability of the structure and of the phase composition. It is known [1] that commercial high-alloy corrosion-resistant austenitic alloys of the Ni – Fe – Cr – Mo system often contain carbides of types $M_{23}C_6$, M_6C, M_7C_3 and MC, nitrides of types TiN, Cr_2N, carbonitrides M(C, N), intermetallic σ, μ and χ phases, and a Laves phase. Cold plastic deformation (CPD) frequently used to raise the strength accelerates the diffusion under subsequent heating and promotes formation of nuclei of second phases thus raising the susceptibility of the supersaturated γ-solid solution to aging. The change in the density and distribution of crystal structure flaws affects the kinetics of the precipitation of second phases and their morphology. Thus, service of an alloy at an elevated temperature can change substantially the physicochemical and mechanical properties of the material, which is extremely undesirable in virtually any case.

It is obvious that the structural and phase stability of the alloys in operation can be improved by two principally different approaches, namely,

(1) optimization of the chemical composition in order to minimize the thermodynamic stimulus to precipitation of second phases and decelerate as much as possible the rate of their formation;

(2) preliminary aging at a temperature exceeding somewhat the maximum operating temperature in order to create a

[1] Ural Federal University after the Fist President of Russia B. N. Eltsyn, Ekaterinburg, Russia (e-mail: s.v.belikov@urfu.ru).

TABLE 1. Chemical Compositions of Studied Alloys

Alloy	Content of elements, wt.%						
	C	Mn	Cr	Mo	Ni	Fe	Remainder
1	0.02	1.48	28.46	3.06	29.48	Base	0.11 Nb; 0.99 Cu; 0.11 Si; 0.04 N; 0.0045 S; 0.0067 P
2	0.02	0.83	25.60	3.20	31.00	Base	1.30 Cu; 0.04 Al; 0.05 Nb; 0.06 Ti; 0.10 W; 0.20 Si; 0.009 S; 0.003 P
3	0.05	–	33.60	8.60	56.20	1.20	0.15 Al; 0.20 Si

distribution of second phases providing the required stability of the alloy.

The aims of the present work were

(1) to analyze the applicability of the active criteria of estimation of metastability of austenite for predicting the operating capacity in the range of up to 500 – 650°C for high-alloy corrosion-resistant iron- and nickel-base alloys in a single-phase preliminarily hardened condition;

(2) to identify the second phases precipitated from the supersaturated austenite under artificial aging of preliminarily hardened high-alloy corrosion-resistant alloys based on Ni and Fe and to determine the temperature and time ranges of their formation;

(3) to determine the effect of preliminary CPD on the kinetics and morphology of the precipitation of particles of second phases.

METHODS OF STUDY

We studied specimens of three high-alloy austenitic alloys the chemical compositions of which are presented in Table 1. Alloys *1* and *2* were melted in an open induction furnace; alloy *3* was melted in a vacuum furnace.

The initial treatment of the iron-base alloys consisted of hot plastic deformation at 1200°C and subsequent cooling in air. The nickel-base alloy was subjected to hardening for austenite at 1135°C. The cold plastic deformation was performed by rolling in flat rolls with strain $e = \ln(l_f/l_0)$ from 0.1 to 1.0, where l_0 is the initial length of the specimen and l_f is the length of the specimen after the rolling.

To study the phase stability during heating of the alloys in preliminarily deformed, quenched and cold-deformed conditions, the specimens were annealed at 550 – 1050°C at a step of 50°C with a hold for 2 – 120 min.

The metallographic analysis was performed with the help of a Jeol JSM 6490-LV scanning electron microscope and a Zeiss Auriga CrossBeam electron-ion microscope in the mode of back-scattered electrons (orientation-composition contrast).

The transmission study of thin foils and the local chemical analysis were performed using a Jeol "JEM-2100" transmission electron microscope (TEM) with an InkaEnergyTEM 250 attachment for microanalysis at an accelerating voltage of 200 kV (136-eV resolution). The foils for the TEM were prepared directly in the chamber of the Zeiss Auriga CrossBeam electron-ion microscope with focused ion beam. The study was performed at the laboratory for structural methods of research and properties of materials and nanomaterials of the UrFU.

RESULTS AND DISCUSSION

Let us consider the possibilities of different approaches to raising the structural and phase stability in multicomponent austenitic alloys based on Fe – Cr – Ni and Ni – Cr – Mo. The phase equilibria in these ternary systems have been studied well enough. We will analyze the concentration-temperature range of the existence of austenite with the help of isothermal sections of the ternary diagrams [2 – 6]. For this purpose we will consider the projections of the austenite region onto the concentration triangle (Fig. 1).

In both systems at 800 – 500°C austenite forms on the base of nickel. The limiting solubility of iron in nickel is much higher than that of molybdenum. Decrease of the temperature from 800 – 750°C to 500°C decreases the solubility from about 95 and about 16 at.% to about 70 and about 6 wt.% for Fe and Mo, respectively. The solubility of chromium changes from about 39 to about 24 at.%. Thus, the ratio of the areas of the γ-region on the isothermal sections of the ternary diagrams is approximately 1 : 6 in favor of the Fe – Cr – Ni system at all the temperatures studied.

Joint analysis of the compositions of commercial high-alloy corrosion-resistant alloys based on nickel and iron and of the phase diagrams of the Fe – Cr – Ni and Ni – Cr – Mo systems shows that an overwhelming majority of them transfers to an austenitic condition at elevated temperatures (1000 – 1200°C); in the range of 500 – 650°C they have a multiphase equilibrium structure and therefore are susceptible to aging.

The susceptibility to precipitation of excess phases from complexly alloyed fcc solid solutions based on iron and nickel is often decisive for determining the operating capacity of corrosion-resistant and refractory alloys and is evaluated in terms of several well-reputed criteria.

Generalization of empirical data has resulted in creation of a State Standard of the RF [7] determining the rules for testing metals for intercrystalline corrosion. This Standard stipulates performance of a provoking annealing at 550, 650, 700 and 1100°C for 20 – 60 min (depending on the grade of the alloy) before the test to cause precipitation of excess

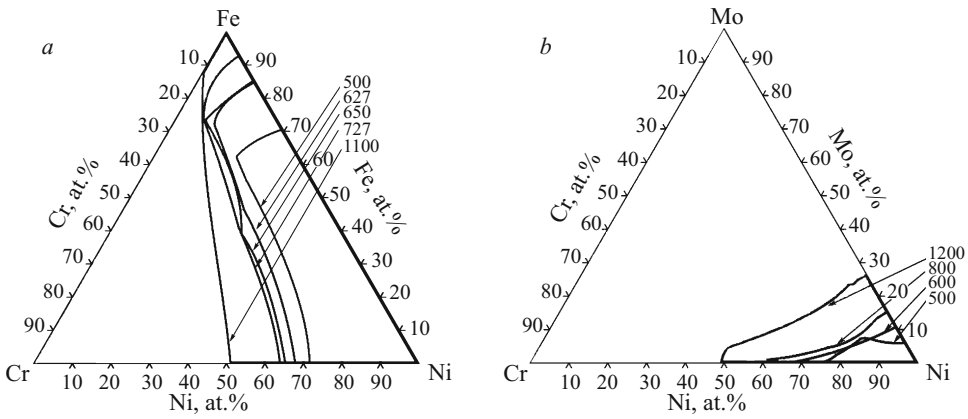

Fig. 1. Temperature-concentration range of existence of nickel-base fcc solid solution in alloys of the Fe – Cr – Ni (*a*) and Ni – Cr – Mo (*b*) systems.

phases over boundaries of austenite grains. If required, the provoking annealing may be performed in another mode, but the choice of the modes is not regulated in the Standard. The very slow kinetics of formation of the majority of tcp phases makes the method mentioned useless for estimating the long-term operating capacity of alloys at elevated temperatures.

Computational curves may be divided into three groups according to the degree of allowance for various factors, namely, allowance for only atomic or mass fraction of the components of the alloy, additional allowance for the number of electrons on the external shells or of electron holes, additional allowance for the atomic mass of the elements, atomic sizes, etc. Computer systems for thermodynamic design of phase diagrams based on CALPHAD have also been developed intensely recently.

It has been shown in [8] that the probability of the appearance of σ-phase in alloys of type KhN30MDB lowers upon growth in the ratio of the content of nickel to the total content of chromium and molybdenum (in wt.%), i.e.,

$$K = [\mathrm{Ni}]/([\mathrm{Cr}] + [\mathrm{Mo}]). \quad (1)$$

$K = 1$ is a critical value. Purposeful increase of K to 1.08 has made it possible to create an alloy with enhanced adaptability to manufacture (alloy *2* in Table 1) due to deceleration of the rate of precipitation of the intermetallics. However, preliminary cold plastic deformation of this alloy accelerates the aging processes, and intermetallics are detected even after a relatively short hold at 750 – 1000°C.

The second group of design criteria is based on the assumption that the austenite of the alloy is the more steady the more distant is the average concentration of electrons on its external electron shells and of electron holes from the concentration typical for intermetallics belonging to the class of electron compounds. For the alloys studied the average concentration of electrons on the *s*- and *d*-sublevels of the external shells is

$$\overline{N}_e = \sum C_i E_i , \quad (2)$$

where E_i is the number of the *sd*-electrons of the *i*th component and C_i is the atomic fraction of the components.

The mean number of holes in the alloys studied is

$$\overline{N}_v = \sum C_i N_{vi} , \quad (3)$$

where N_{vi} is the number of holes for the *i*th component. Computation of $\overline{N}_v$ has become the basis of the commercial Facomp method (it is sometimes termed the Facomp parameter) [9]. In the general case the choice of the critical value of $\overline{N}_e$ and $\overline{N}_v$ (N_e and N_v) is made empirically for each group of alloys individually. In the Facomp method the critical value is assumed to be $N_v \le 2.45 – 2.50$ [10], but the authors stress that for some grades of alloys this value should be corrected with allowance for experimental data. In fact, this transfers the hole concentration of individual elements to the category of fitting coefficients. This especially concerns molybdenum to which $N_v = 4.66 – 10$ is assigned depending on the composition of the alloy.

Specialists of the All-Russia Institute for Aircraft Materials (FGUP "VIAM") have suggested [10] an empirical formula of alloying balance for refractory nickel alloys to characterize the ultimate joint solubility of substitutional elements in a nickel matrix, i.e.,

$$\Delta E = \sum E_i C_i – (0.036 \sum A_i C_i + 6.28), \quad (4)$$

where ΔE is the parameter of alloying disbalance, A_i and E_i are the atomic mass and the number of the *sd*-electrons of the *i*th component, respectively, and C_i is the atomic fraction of the component. Criterion $– 0.02 \le \Delta E \le 0.02$ of stability of austenite is common for all compositions. Advancement of this approach has made it possible to create a method of balanced alloying for refractory nickel alloys, and its seems expedient to estimate is applicability for developing austenitic alloys with elevated corrosion resistance.

To check the adequacy of the criteria considered we should determine the phase composition of the alloys in quenched condition and after aging. We chose the quenching temperature after analyzing isothermal sections of the phase diagrams and the results of our previous works [8] for obtaining a single-phase austenitic structure.

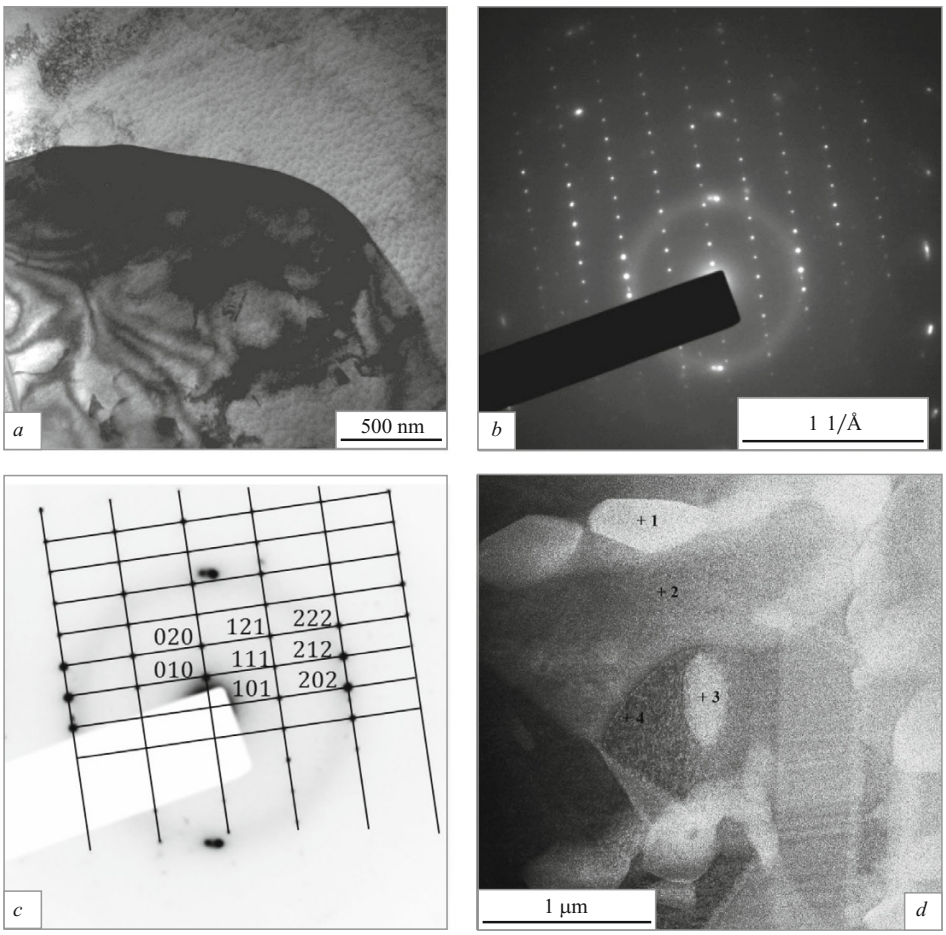

Fig. 2. A particle of σ-phase (axis of zone [$\bar{1}$02]) in alloy *3*. Annealing at 1000°C for 4 h: *a*) light-background image; *b*) micro diffraction; *c*) deciphering of the microdiffraction; *d*) TEM.

Using the metallographic method we established that in the quenched condition all the three alloys had an austenitic structure with a mean grain size of 70 – 150 μm and annealing twins; the iron-base alloys contained some coarse edged particles of carbonitrides (Ti, Nb)(C, N).

It has been shown in [8] that alloys *1* and *2* are susceptible to precipitation of σ-phase in aging, which has an average composition $Fe_{32}Ni_{15}Cr_{47}Mo_6$. Deciphering of microdiffraction patterns allowed us to determine the orientation relation $(–11–1)_\gamma // (00–1)_\sigma$, $[110]_\gamma // [–410]_\sigma$, and an x-ray diffraction phase analysis of the electrolytic precipitate gave us the lattice constants of the detected phase, i.e., $a = 0.882$ nm and $c = 0.458$ nm.

TABLE 2. Chemical Composition of σ-Phase in the Austenite Matrix of Alloy *3*

Studied place	Content of elements, wt.%/at.%			
	Cr	Fe	Ni	Mo
σ-phase (points *1* and *3* in Fig. 2)	46/53	1/1	32/33	21/13
Austenite matrix (point *2* in Fig. 2)	33/37	2/2	58/57	7/4

It is known that many nickel alloys of the Ni – Cr – Mo – (Fe) system are also susceptible to formation of topologically close-packed intermetallic phases during aging [11 – 13]. The alloys with compositions close to that of alloy *3* (Table 1) have been shown to contain σ- and μ-phases with body-centered tetragonal and rhombohedral lattices. The type of the precipitated phase depends on the content of molybdenum; the higher the latter, the greater the probability of formation of μ-phase. In the present work alloy *3* also showed a tendency to formation of σ-phase at $T_{an} = 600 – 1000$°C (Fig. 2); the chemical composition of its particles is presented in Table 2.

Minimum time to the start of formation of excess σ-phase in the whole of the temperature range studied is typical for alloy *1*; alloy *2* is the most stable, and alloy *3* takes an intermediate position.

When computing the criteria of stability of austenite in the alloys by formulas (1) – (4) we based ourselves on the following criteria:

– in quenched condition the austenite composition matches the standardized one (Table 1) except for the contents of carbon, titanium and niobium;

– the influence of Si, S, P, Al, Co, Mn and Cu may be neglected due to their inconsiderable presence; Ti and Nb are bonded in carbides/carbonitrides of type MC/M(C, N);

TABLE 3. Parameters of the Main Components of Studied Alloys [10, 11]

Element	E_i	N_{vi}	A_i
Cr	6	4.66	52.00
Mo	6	10.00	95.94
Fe	8	2.22	55.85
Ni	10	0.61	58.71

TABLE 4. Criteria of Stability of Austenite in Studied Alloys

Alloy	K_c	$\overline{N}_e$	$\overline{N}_v$	ΔE
1	0.94	7.91	2.67	– 0.40
2	1.08	8.00	2.57	– 0.30
3	1.33	8.26	2.65	– 0.11

– the computation is performed with respect to Ni, Fe, Cr and Mo;

– σ-phase precipitates in the aging process directly from the austenite;

– the probable number of *sd*-electrons and electron holes is as that given in Table 3.

The results of the computation are presented in Table 4. Let us analyze these data. In the iron-base alloys parameter Kc grows with the content of nickel, but the susceptibility to formation of σ-phase is preserved.

The value of K_c can be estimated roughly with allowance for the isothermal sections of the Fe – Cr – Ni diagram. At 650°C the solvus line in the range of the compositions studied corresponds to the alloys with $K_c \approx 1.25$; at 500°C it corresponds to the alloys with $K_c \approx 2.11$. In the Ni – Cr – Mo system the range of stable austenite, which is rather wide at high temperatures, narrows markedly at 500 – 650°C. Cooling of alloy *3*, which is austenitic at 1200°C, to 600°C transfers it to a two-phase condition. In the alloy studied the ratio of the content of chromium to that of molybdenum is about 7; an austenitic alloy, which is single-phase a 600°C and has the same ratio, should contain at most 23% Cr, 3% Mo, and at least 74% Ni at $K_c = 2.85$, i.e., despite the higher absolute value of K_c the nickel alloy becomes less stable than the iron alloys at relatively low temperatures.

The mean number density of *sd*-electrons in electron compounds should be close to 7 [14], which agrees well with the computed data for the tcp phases detected both in the iron alloys and in the nickel one. Growth of $\overline{N}_e$ in the iron-base alloys results in the expected growth of their stability. However, nickel alloy *3* with the highest number density of *sd*-electrons takes an intermediate position with respect to the stability of the austenite.

Accordingly, the hole number density $\overline{N}_v$ in alloys *1*, *2* and *3* is 9, 5 and 8% higher that the accepted critical value of 2.45. However, the evaluation by the Facomp method is more informative, because it reflects the correctly the stability of the alloys.

The value of ΔE for all the three alloys is negative and is outside the admissible limits, which reflects disbalance of their alloying and their enhanced susceptibility to formation of compounds of type M_6C and tcp phases like μ and σ.

Thus, we have shown that only the $\overline{N}_v$ and ΔE computational criteria of stability of austenite characterize appropriately the inapplicability of the studied corrosion-resistant alloys to service at elevated temperatures in quenched condition, the nature of the excess phase, and the comparative resistance of the austenite to its formation. In addition, the universal critical value $-0.02 \le \Delta E \le 0.02$ [10] of disbalance of alloying allows us to compute the composition of a matrix that should posses enhanced stability.

Simultaneous increase in the content of nickel and decrease in the content of chromium and molybdenum in the austenite raises its resistance to formation of σ-phase. On the other hand, precipitation of an σ-phase enriched with chromium and molybdenum and depleted of nickel should stabilize the matrix. Taking this into account we can easily compute the composition of the matrix and the respective content of σ-phase (Table 5).

Note that the results of the computation (Table 5) can be used to compute the corresponding critical values of the Facomp parameter, i.e., 2.45 – 2.47 for alloys *1* and *2* and 2.46 – 2.52 for alloy *3*. The Facomp parameter of the austenite matrix near an inclusion of σ-phase in alloy *3* computed with the use of the data of the microscopic x-ray diffraction analysis (Table 2) ranges within $\overline{N}_v = 2.49$. The content of the σ-phase determined metallographically is 10 ± 2 vol.% and also agrees with the computation.

Thus, the parameter of disbalance of alloying ΔE turns out to be the most convenient and informative not only for developing and correcting the compositions for promising alloys but also for choosing the aging modes for metastable alloys. However, the criteria considered do not concern such

TABLE 5. Balanced Composition of the Austenite Matrix and Content of σ-Phase Required for Its Formation

Alloy	Chemical composition of austenite, wt.%				Content of σ-phase, vol.%
	Ni	Fe	Cr	Mo	
1, *2*	44.04 – 42.83	31.79 – 31.80	21.51 – 22.57	2.66 – 2.80	18.7 – 15.2
3	59.87 – 58.76	1.23 – 1.22	32.01 – 32.56	6.89 – 7.45	12.3 – 8.7

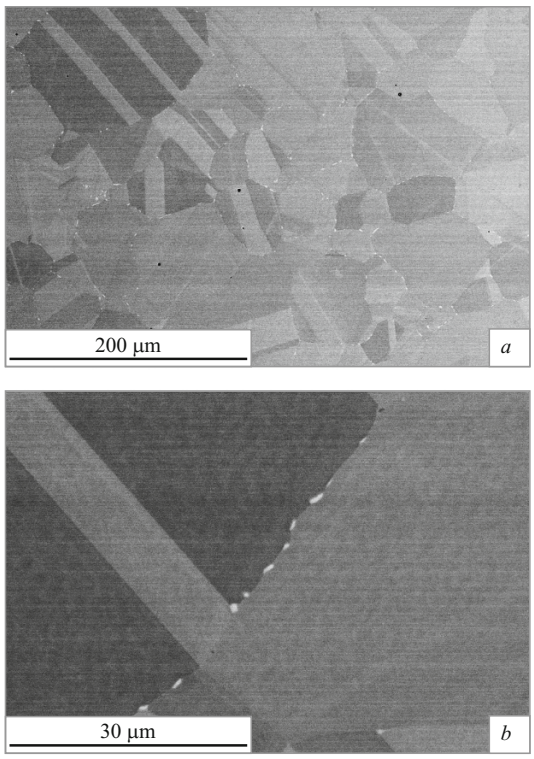

Fig. 3. Chains of particles of σ-phase on boundaries of austenite grains in alloy *3* after 4-h annealing at 1000°C.

principally important characteristics as the morphology and kinetics of precipitation of excess phases.

In all the three alloys the σ-phase has the same morphology (Fig. 3). Lamellar particles nucleate over boundaries of austenite grains. Annealing twins do not become places of preferential nucleation.

It is known from publications [2 – 6] that the type of precipitated excess phases in alloys with compositions studied may change at a relatively low temperature. Lowering of the aging temperature to 600°C complicates the picture of decomposition of supersaturated austenite in alloy *3*; the σ-phase is accompanied by near-boundary chains of particles of another excess phase (Fig. 4). Judging by the electron diffraction patterns these particles have a bcc lattice with parameter $a = 0.29 \pm 0.01$ nm. In our opinion, these particles should be an α-Cr solid solution. Individual particles also occur in bodies of γ-grains (Fig. 4*b*). The dark color of the inclusions in the images of microstructure in the orientation-composition contrast implies that their mean atomic mass is smaller that that of the austenite matrix. The results of the XRDA and TEM show that these particles are enriched with chromium and molybdenum at simultaneous decrease in the nickel concentration (Table 6).

Further efforts were directed at substantiating and developing expedient modes of deformation-heat treatment of corrosion-resistant alloys. We posed the following tasks: to change the morphology of the particles of σ-phase from lamellar to a fine equiaxed one, to provide their uniform distribution in the austenite matrix, and to provide an admissible duration of heat treatment due to easier nucleation and growth. The three tasks can be solved by changing the places

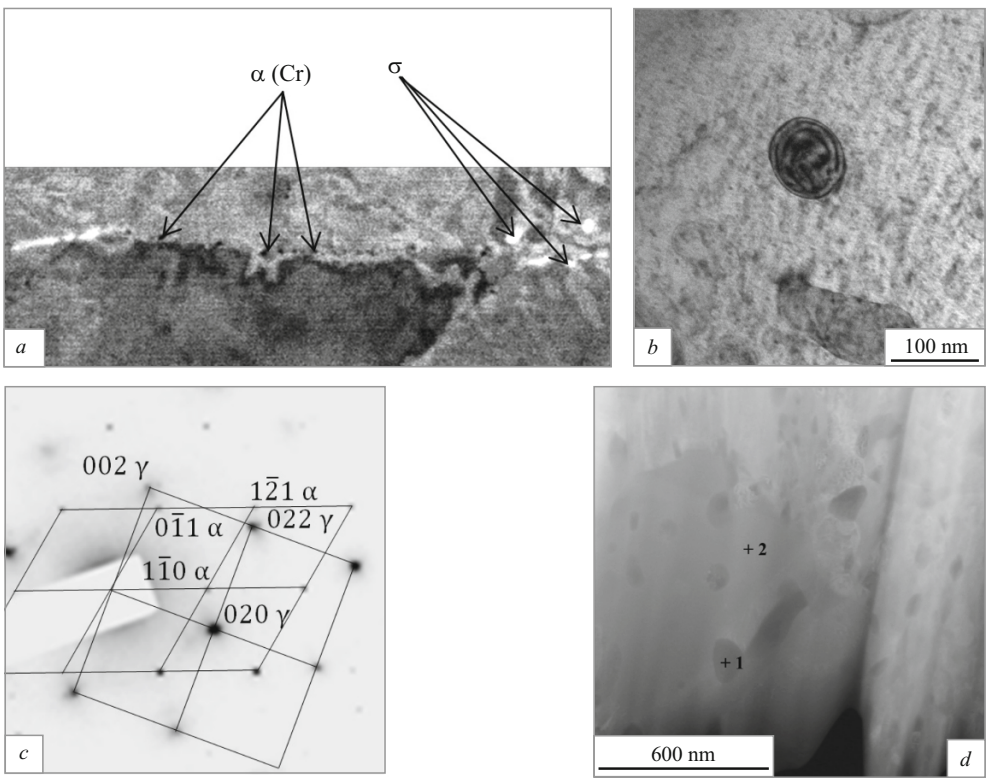

Fig. 4. Particles of α-Cr in alloy *3* after 0.5-h annealing at 900°C: *a*, *b*) over boundaries and in bodies of austenite grains, a light-background image; *c*) microdiffraction and its deciphering, zones $[111]_{\alpha\text{-Cr}}$ and $[100]_{\gamma}$; *d*) TEM.

TABLE 6. Chemical Composition of the Solid Solution Based on α-Cr and of the Austenite Matrix

Place of study	Content of elements, wt.%/at.%			
	Cr	Fe	Ni	Mo
α-Cr (point *1* in Fig. 4*d*)	77/83	1/1	9/8	13/8
Austenite matrix (point *2* in Fig. 4*d*)	29/32	1/1	62/62	8/5

of preferable nucleation σ-phase particles by raising the density of defects of the crystal structure of the austenite with the help of preliminary cold plastic deformation (CPD) under the condition that the precipitation of the excess phases on the defects would precede the recrystallization and by choosing an appropriate aging temperature. The uniformity of the deformation over cross section and hence of the morphology of the precipitated excess phases depends on the degree of the deformation, its stages, and the variant of application of the load. Nucleation in a not deformed or weakly deformed alloy at any temperature occurs over triple intersections and on high-angle boundaries. With time, inclusions start to nucleate on defects and in the body of austenite grains; thin-plate precipitates form after a long-term hold. The intragrain nucleation accelerates with growth of the temperature.

When the degree of the CPD is increased, the places of preferential nucleation of excess phases change. When the density of the crystal structure defects increases, the temperature of the start of recrystallization falls markedly, but in the range of 800 – 850°C the process of precipitation of excess phases becomes a leading one. Accordingly, in the first stages chains of inclusions form over grain boundaries and over defects in grain bodies (Fig. 5). In some cases the particles grow following a displacing boundary.

At higher temperatures the processes of cell formation and partially of recrystallization precede the start of nucleation. The number of the formed nuclei is little, they are distributed more uniformly, and grow rapidly enough (Fig. 6). The high-angle boundaries are hindered by the particles, and the austenite acquires a homogeneous fine-grained structure with uniformly distributed round particles of σ-phase about 0.5 – 1 μm in size.

The results of the metallographic analysis of the changes in the morphology of the σ-phase as a function of the degree of the preliminary CPD and of the annealing mode allowed us to determine some universal rules generalized in the scheme given in Fig. 7. The elongated and round grains of the matrix reflect the deformed and crystallized conditions, respectively.

The study of the kinetics of the precipitation of excess phases (Fig. 8) showed that inconsiderable deformation ($e = 0.1$) accelerates the formation of excess phases at a temperature below the "nose" of the *C*-curve (especially noticeably at 900 – 850°C) in the nickel alloy and in the whole of the temperature range studied in the iron-base alloys virtu-

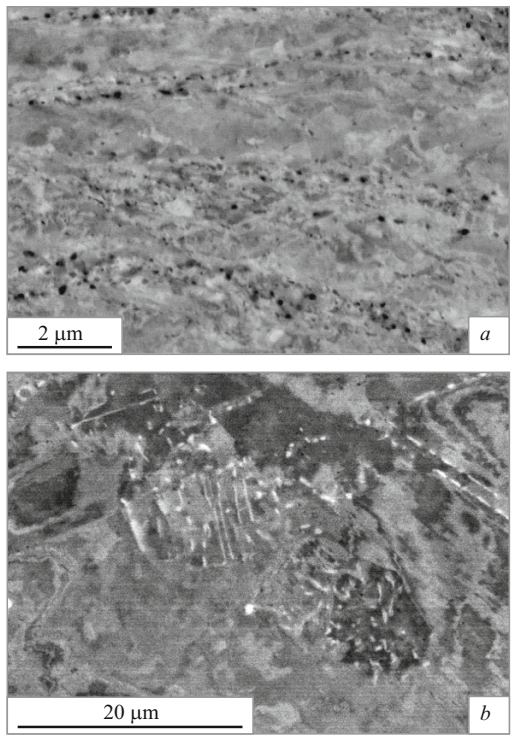

Fig. 5. Particles of excess phases on flaws in alloy *3*: *a*) 30-min annealing at 775°C, $e = 1.0$; *b*) 30-min annealing at 900°C, $e = 0.3$.

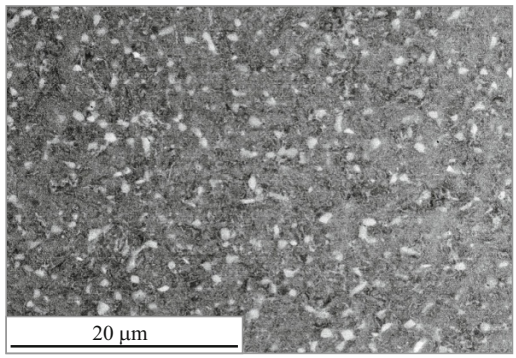

Fig. 6. Particles of excess phases in alloy *3* after annealing at 975°C for 30 min ($e = 1.0$).

ally without changing the morphology. We established that the nucleation of particles of α-Cr and of the σ-phase developed independently. Intensification of the CPD accelerated the precipitation of α-Cr much more that that of the σ-phase due to the low temperature of its precipitation. For example, increase of the degree of preliminary cold plastic deformation from 0.1 to 1.0 shortened the minimum incubation period from 15 to 6 min. Deformation with degree $e = 1.0$ widened the range of formation chromium-base solid solution to 550°C.

Considerable increase in the degree of CPD affects the stability of the austenite in the iron-base alloys. When it is raised from 0.4 to 1.2, the time τ_{min} decreases by almost a

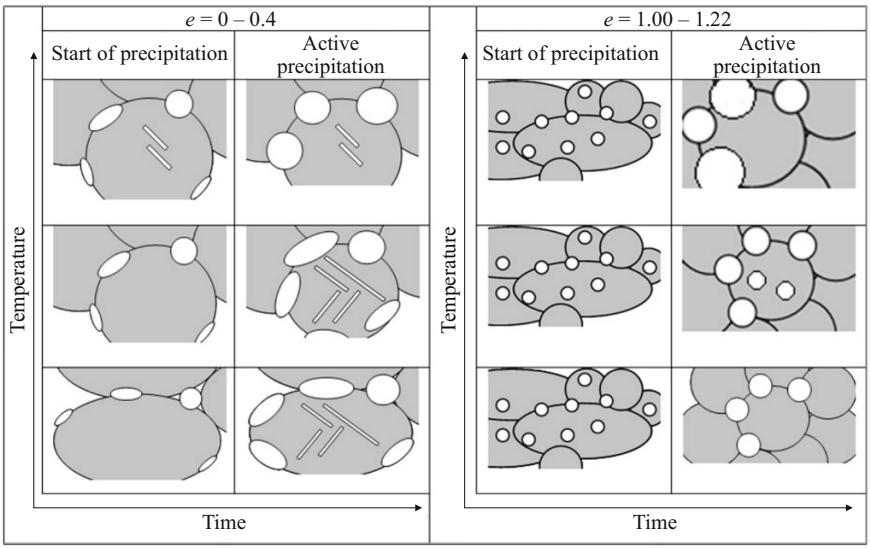

Fig. 7. Scheme of changes in the morphology of precipitation of σ-phase as a function of the degree of the CPD of the alloy, of the temperature, and of the annealing time.

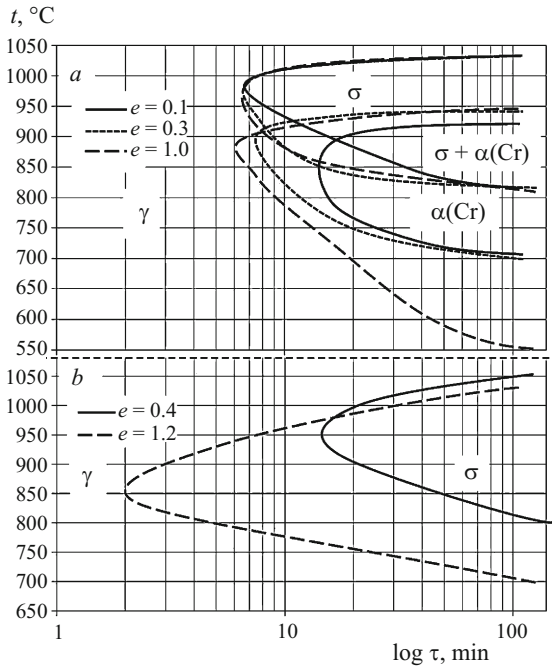

Fig. 8. Kinetics of precipitation of excess phases as a function of the degree of preliminarily CPD: *a*) alloy *3*; *b*) alloy *2*.

factor of 7 (from 15 to 2 min), and the temperature of minimum stability of the austenite decreases by 100°C (from 950 to 850°C); the temperature range of precipitation of σ-phase widens by the same value due to shifting of the lower branch of the *C*-curve to the left.

The laws of precipitation of excess phases determined in the present work allow us to make an appropriate choice of the mode of preliminary cold plastic deformation and subsequent aging of the alloys in order to create different structural states. The most promising kind of structure for steady and enhanced corrosion resistance of the alloys at high operating temperatures is a two-phase γ + σ structure with equiaxed fine and uniformly distributed intermetallic particles and austenite with a balanced chemical composition.

CONCLUSIONS

1. The main intermetallic phase precipitating in corrosion-resistant high-alloy austenitic alloys based on Fe and Ni in the temperature range of 700 – 1050°C is a σ-phase. The average composition of this phase in iron-base alloys is $Fe_{32}Ni_{15}Cr_{47}Mo_6$; in nickel-base alloys it is $FeNi_{33}Cr_{53}Mo_{13}$. In a not deformed condition the σ-phase precipitates on high-angle boundaries and has a lamellar shape. In addition to the σ-phase, fine round particles of an α-Cr-base solid solution precipitate over grain boundaries in nickel-base alloys in the range of 550 – 950°C.

2. Low degrees of deformation (e = 0.1 – 0.4) do not affect substantially the morphology of the σ-phase in the initial stages of the precipitation: lamellar particles form over grain boundaries; long holds result in formation of intragrain lamellar precipitates growing over planes (111) of the austenite. Increase in the degree of deformation (e = 0.5 – 1.22) raises the density of defects and hence the number of nucleation centers. This provides lowering of the mean size of the particles and their more uniform distribution. The shape of the particles changes for an equiaxed one and is preserved during aging.

3. Studying the effect of preliminary cold plastic deformation on the kinetics of precipitation of excess phases we plotted parts of *C*-curves for the temperature range of 550 – 1050°C. Growth in the degree of preliminary cold plastic deformation (e = 0.1 – 1.0) in the nickel-base alloy accelerated considerably the precipitation of the α-Cr-base solid solution (the minimum incubation period shortened from 15 to 6 min). In the iron-base alloys increase in the degree of preliminary cold plastic deformation from 0.4 to 1.2

shortened the incubation period of formation of σ-phase from 15 to 1 min and reduced the temperature of the "nose" of the corresponding *C*-curve from 950 to 850°C.

4. The parameter of alloying disbalance Δ*E* has been used to determine a balanced composition of the austenite matrix and the content of σ-phase required to attaining this composition. For the iron-base alloys we suggest (in wt.%) (44.04 – 42.83) Ni, (31.79 – 31.80) Fe, (21.51 – 22.57) Cr and (2.66 – 2.90) Mo; the content of the σ-phase should be 18.7 – 15.2 vol.%. For the nickel-base alloy the figures are (in wt.%): (59.87 – 58.76) Ni, (1.23 – 1.22) Fe, (32.01 – 32.56) Cr and (6.89 – 7.45) Mo; the content of the σ-phase is 12.3 – 8.7 vol.%.

REFERENCES

1. F. F. Khimushin, *Stainless Steels* [in Russian], Metallurgiya, Moscow (1967), 800 p.
2. F. H. Hayes, M. G. Hetherington, and R. D. Longbottom, "Thermodynamics of duplex stainless steels," *Mater. Sci. Technol.*, **6**, 263 – 272 (1990).
3. G. V. Raynor and V. G. Rivlin, *Cr – Fe – Ni Phase Equilibria Iron Ternary Alloys*, Inst. Met., London (1988), pp. 316 – 332.
4. J. A. Golczewski, H. L. Lukas, M. Bamberger, et al., "Phase diagrams of the Ni – Fe – Mo and Ni – Cr – Mo ternary systems — experiments and thermodynamic calculations as a basis of superalloy development," in: *Adv. Mater. Processes, Proc. Eur. Conf. 1st* (1990), pp. 365 – 370.
5. K. P. Gupta, "The Cr – Mo – Ni (chromium-molybdenum-nickel) system. Phase diagrams of ternary nickel alloys," *Indian Inst. Metals*, **1**, 26 – 48 (1990).
6. P. E. A. Turchi, L. Kaufman, and Z. K. Liu, "Modeling of Ni – Cr – Mo based alloys. Part I – phase stability," *CALPHAD: Comput. Coupling Phase Diagrams Thermochem.*, **30**, 70 – 87 (2006).
7. *GOST 6032–2003, Corrosion-Resistant Steels and Alloys. Methods for Testing for Resistance to Intercrystalline Corrosion* [in Russian].
8. A. A. Popov, A. S. Bannikova, and S. V. Belikov, "Precipitation of σ-phase in high-alloy austenitic chromium-nickel-molybdenum alloys," *Fiz. Met. Metalloved.*, **108**(6), 1 – 8 (2009).
9. G. T. Sims, N. S. Stoloff, and W. C. Hagel, *Superalloys II: Refractory Materials for Aerospace and Industrial Plants* [Russian translation], Metallurgiya, Moscow (1995), 384 p.
10. G. I. Morozova, "Compensation of disbalance of alloying of refractory nickel alloys," *Metalloved. Term. Obrab. Met.*, No. 12, 52 – 6 (2012).
11. D. M. E. Villanueva, F. C. P. Junior, R. L. Plaut, and A. F. Padilha, "Comparative study on sigma phase precipitation of three types of stainless steels: austenitic, superferritic and duplex," *Mater. Sci. Technol.*, **22**(9), 1098 – 1104 (2006).
12. J. Anburaj, S. S. M. Nazirudeen, R. Narayanan, et al., "Ageing of forged superaustenitic stainless steel: precipitate phases and mechanical properties," *Mater. Sci. Eng. A*, **535**(15), 99 – 107 (2012).
13. T. Koutsoukis, A. Redijaimia, and G. Fourlaris, "Phase transformations and mechanical properties in heat treated superaustenitic stainless steels," *Mater. Sci. Eng. A*, **561**(20), 477 – 485 (2013).
14. J.-M. Joubert, "Crystal chemistry and Calphad modeling of the σ-phase," *Progr. Mater. Sci.*, **53**, 528 – 583 (2008).